



Title	Effects of Welding Residual Stresses and Initial Deflection on Rigidity and Strength of Square Plates Subjected to Compression
Author(s)	Ueda, Yukio; Yasukawa, Wataru; Yao, Tetsuya et al.
Citation	Transactions of JWRI. 1975, 4(2), p. 133-147
Version Type	VoR
URL	https://doi.org/10.18910/11190
rights	
Note	

The University of Osaka Institutional Knowledge Archive : OUKA

<https://ir.library.osaka-u.ac.jp/>

The University of Osaka

Effects of Welding Residual Stresses and Initial Deflection on Rigidity and Strength of Square Plates Subjected to Compression[†]

Yukio UEDA*, Wataru YASUKAWA**, Tetsuya YAO*** Hiroshi Ikegami** and Ryoichi OHMINAMI**

Abstract

When structures are constructed by welding, structural elements are always accompanied by welding residual stresses and usually also by deformation. Therefore, when the rigidity and strength of the welded structures are considered, it is very important to have sufficient information about the effects of initial deflection and welding residual stresses on them. In this paper, as a fundamental study on this matter, the square plates under compression are dealt with. At first, two series of experiments were conducted, one using the specimens with initial deflection, and the other using the specimens with initial deflection and welding residual stresses. The specimens are 500 x 500 mm square plates of which thicknesses are 4.5mm, 9.0mm and 12.7mm, and are simply supported along the four edges. Secondly, a series of the elastic-plastic large deflection analysis was carried out by the finite element method in order to clarify the effects of the shape of initial deflection, the magnitude of initial deflection, and welding residual stresses with initial deflection. It was found that the initial deflection and residual stresses reduce the rigidity and ultimate strength and this tendency becomes larger for thicker plates.

1. Introduction

In general, steel structures are fabricated by welding, and structural elements are always accompanied by welding residual stresses and usually also by deformation. These influence performance of the welded structures. Therefore, it is very important to have sufficient and accurate information about effects of these welding imperfections on the rigidity and strength of structural elements, for more accurate evaluation of performance of the welded structures containing these imperfections.

Concerning the effect of initial deflection, Yamamoto¹⁾ proposed a theory on the plastic buckling strength of a plate under compression. Yoshiki et al.²⁾ dealt also with buckling strength and corrugation of continuous panel with initial deflection under compression, and Fukumoto³⁾ studied the rigidity of the continuous panel with initial deflection under compression, tension and bending. As to the effect of welding residual stresses, Yoshiki et al.,⁴⁾ Fujita et al.,⁵⁾ Ueda et al.⁶⁾⁷⁾ and Ueda⁸⁾ dealt with local buckling strength of I-section plate column or box plate column which are composed by welding. Although the buckling strength was evaluated as the solution of a characteristic equations, in the strict sense, the elastic-plastic large deflection analysis was not carried out in these studies.

Recently, owing to remarkable development in digital computers, possibility of analysis of the elastic-plastic large deflection problems has been shown, and

several examples are analysed.⁹⁻¹²⁾ However, so far information is not adequate about the effects of the welding residual stresses and initial deflection on the rigidity and strength of welded structures.

In this paper, as a fundamental study on this matter, the behavior of simply supported square plates subjected to compression is investigated.¹³⁾

First, two series of experiments are conducted; one to examine effect of initial deflection, and the other to combined effects of initial deflection and welding residual stresses. Then, the elastic-plastic large deflection analysis is carried out using the finite element method of which the formulation of the analysis was developed by one of the authors. By this analysis, effects of the shape of initial deflection, the magnitude of initial deflection and the welding residual stresses on the rigidity and strength of the compressive square plates are studied. Also, the relation between welding residual stresses and the welding deformation is examined.

2. Experiment

2.1 Test Specimens

Test specimens are 500 x 500mm square plates of which thicknesses are 4.5mm, 9.0mm and 12.7mm. The material of the specimen is mild steel (SM 41). When the specimens, simply supported along the edges, are subjected to uniaxial compression, their theoretical buckling stresses are 0.21, 0.75 and 1.00 times the yield stress, respectively.

[†] Received on July 28, 1975

* Associate Professor

** Akashi Technical Research Institute, Kawasaki Heavy Industry, Ltd.

*** Research Associate

made as shown in Fig. 3. The compressive load is applied with the aid of the Amsler type testing machine. In the experiment, the strains are measured using the foil strain gauges in three directions, and the deflections are also measured using dial gauges.

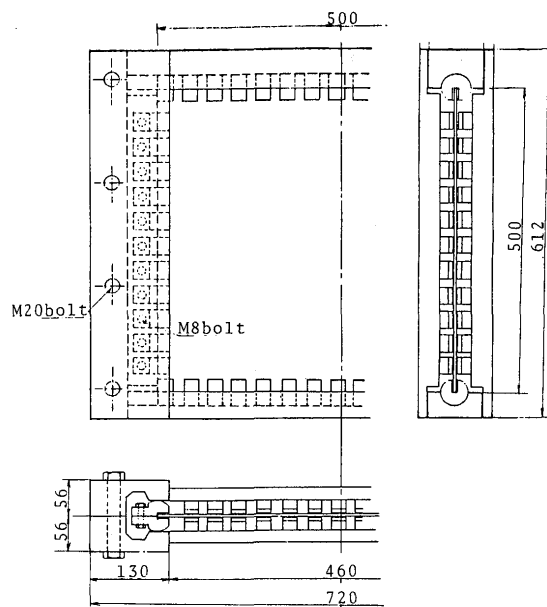


Fig. 3 Load frame and end fixture.

2.4 Test results

The test results are summarized in Table 2. It is noted from the results that both initial deflection and welding residual stresses decrease the ultimate strength of the plates under compression.

In this section, the behaviours of the square plates under compression are mainly discussed based on test results, and the ultimate strength will be compared with the results of analysis by the finite element method in Chapter 4.

Figs. 4(a), (b) and (c) show relations between the average compressive stress and the central deflection of several specimens for each plate thickness, respectively. The full lines represent the relation for specimens with initial deflection, and the dotted lines for those with both initial deflection and welding residual stresses. It is seen from these results that the slope of these curves becomes larger by the existence of initial deflection and welding residual stresses. That is, these initial imperfections decrease the rigidity of plates under compression.

Figs. 5(a) and (b) show two typical examples of variation in shape of deflection for a thin plate, C-4.5-1.02 and a thick plate, C-12.7-0.26-1, respectively. In the case of a thin plate, the deflection increases at all parts of the plates simultaneously as the load increases. On the contrary, in the case of a thick plate, the deflection increases at the central portion of the plate,

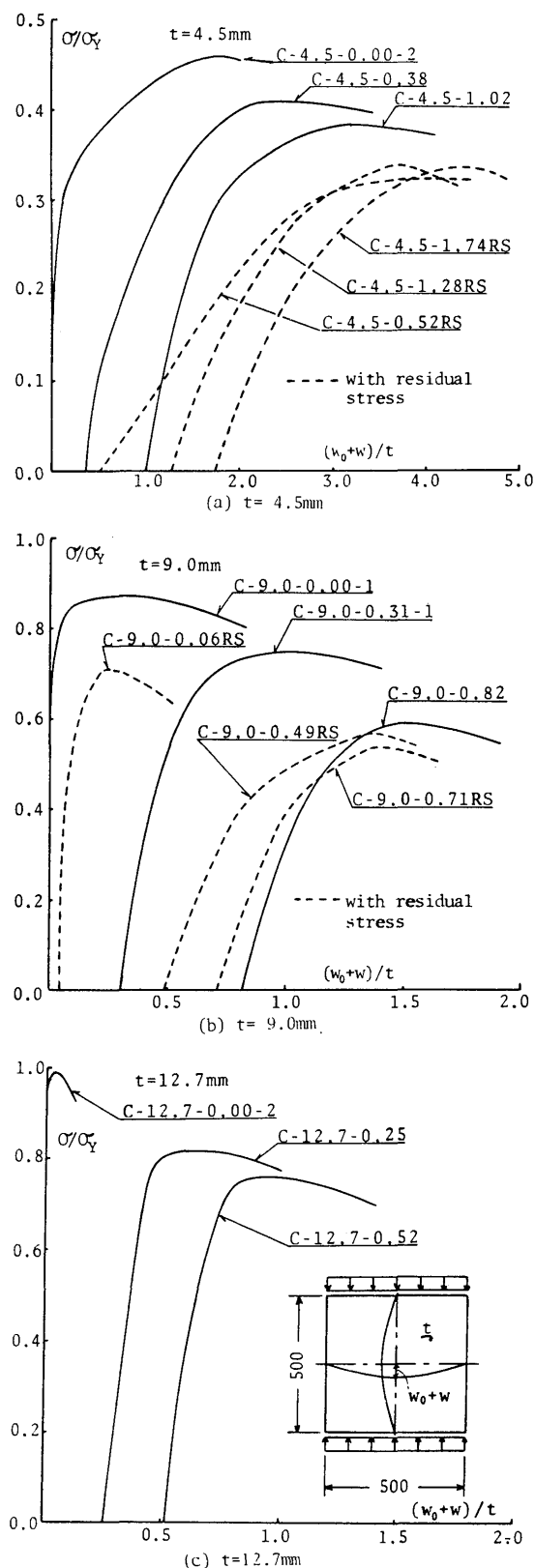


Fig. 4 Applied compressive stress - central deflection curves. (Experiment)

where local plastification proceeds at the early stage of loading. Then, the length of the buckling wave becomes shorter showing the deformation pattern of the roof shape.

Table 2 Details of specimens and Test results

Specimen	Detail of Specimen				Test Results		
	t (mm)	σ_Y (kg/mm ²)	b/t	W_o/t	Pm (tons)	σ_m (kg/mm ²)	σ_m/σ_Y
C-4.5-0.00-1	4.50	28.49	111.11	0.00	25.00	11.11	0.39
C-4.5-0.00-2	4.50	26.59	111.11	0.00	26.90	11.96	0.45
C-4.5-0.09-1	4.50	26.66	111.11	0.09	24.60	10.93	0.41
C-4.5-0.09-2	4.50	26.00	111.11	0.09	26.90	11.96	0.46
C-4.5-0.09-3	4.50	25.87	111.11	0.09	26.20	11.64	0.45
C-4.5-0.24	4.50	26.27	111.11	0.24	26.00	11.56	0.44
C-4.5-0.27	4.50	28.07	111.11	0.27	25.90	11.51	0.41
C-4.5-0.31	4.50	26.45	111.11	0.31	25.00	11.11	0.42
C-4.5-0.36	4.50	26.88	111.11	0.36	25.40	11.29	0.42
C-4.5-0.38	4.50	26.66	111.11	0.38	24.60	10.93	0.41
C-4.5-0.89	4.50	28.03	111.11	0.89	24.60	10.93	0.39
C-4.5-1.02	4.50	25.16	111.11	1.02	21.50	9.56	0.38
C-4.5-0.33RS	4.34	22.01	115.21	0.33	15.15	6.98	0.32
C-4.5-0.52RS	4.34	22.01	115.21	0.52	15.45	7.12	0.32
C-4.5-1.07RS	4.34	23.42	115.21	1.07	15.30	7.05	0.30
C-4.5-1.28RS	4.34	23.08	115.21	1.28	16.95	7.81	0.34
C-4.5-1.31RS	4.34	21.05	115.21	1.31	15.80	7.28	0.35
C-4.5-1.74RS	4.34	22.87	115.21	1.74	16.63	7.66	0.33
C-9.0-0.00-1	8.80	31.03	56.82	0.00	118.80	27.00	0.87
C-9.0-0.00-2	8.80	31.20	56.82	0.00	116.70	26.52	0.85
C-9.0-0.00-3	8.80	31.06	56.82	0.00	127.10	28.89	0.93
C-9.0-0.00-4	9.00	28.71	55.56	0.00	109.75	24.40	0.85
C-9.0-0.26	8.80	31.96	56.82	0.26	95.60	21.73	0.68
C-9.0-0.31-1	8.80	31.27	56.82	0.31	101.80	23.14	0.74
C-9.0-0.31-2	8.80	30.91	56.82	0.31	102.00	23.18	0.75
C-9.0-0.38	8.80	30.21	56.82	0.38	97.00	20.05	0.73
C-9.0-0.61	8.80	32.11	56.82	0.61	86.20	19.59	0.61
C-9.0-0.68	9.00	28.63	55.56	0.68	81.20	18.04	0.63
C-9.0-0.72	9.00	25.07	55.56	0.72	75.60	16.80	0.67
C-9.0-0.73	8.80	30.53	56.82	0.73	80.60	18.32	0.60
C-9.0-0.75	8.80	30.30	56.82	0.75	80.00	18.18	0.60
C-9.0-0.82	8.80	30.52	56.82	0.82	77.92	17.70	0.58
C-9.0-0.84	9.00	25.39	55.56	0.84	67.40	14.98	0.59
C-9.0-0.02RS	8.85	25.60	56.50	0.02	79.80	18.03	0.70
C-9.0-0.06RS	8.95	26.81	55.87	0.06	84.60	18.91	0.70
C-9.0-0.48RS	8.83	25.28	56.63	0.48	59.80	13.55	0.54
C-9.0-0.49RS	8.70	25.55	57.47	0.49	62.60	14.34	0.56
C-9.0-0.71RS	8.80	25.55	56.82	0.71	61.80	14.05	0.55
C-9.0-0.77RS	8.70	25.55	57.47	0.77	50.00	11.49	0.45
C-12.7-0.00-1	12.80	25.20	39.06	0.00	154.80	24.19	0.96
C-12.7-0.00-2	12.80	25.09	39.06	0.00	159.00	24.84	0.99
C-12.7-0.00-3	12.80	25.09	39.06	0.00	157.40	24.59	0.98
C-12.7-0.00-4	12.80	25.03	39.06	0.00	160.20	25.03	1.00
C-12.7-0.00-5	12.90	30.16	38.76	0.00	192.60	29.86	0.99
C-12.7-0.20	13.30	29.52	37.59	0.20	159.00	23.91	0.81
C-12.7-0.25	13.30	29.51	37.59	0.25	162.96	24.50	0.83
C-12.7-0.26-1	12.90	30.46	38.76	0.26	159.12	24.67	0.81
C-12.7-0.26-2	13.30	29.34	37.59	0.26	160.00	24.06	0.82
C-12.7-0.36	12.91	30.32	38.76	0.36	158.40	24.56	0.81
C-12.7-0.42	13.30	29.47	37.59	0.42	145.00	21.80	0.74
C-12.7-0.43-1	12.90	30.49	38.76	0.43	153.40	23.78	0.78
C-12.7-0.43-2	13.30	29.32	37.59	0.43	140.40	21.11	0.72
C-12.7-0.52	12.90	30.15	38.76	0.52	143.90	22.31	0.74
C-12.7-0.53	12.90	30.29	38.76	0.53	148.50	23.02	0.76

notation of specimen number ; e.g. C-4.5-0.52RS

C: compression, 4.5: plate thickness,
0.52: w_o/t RS: with residual stresst ; plate thickness σ_Y ; yield stress
b ; plate width Pm ; ultimate load
 w_o ; initial deflection $\sigma_m = Pm/tb$; ultimate strength

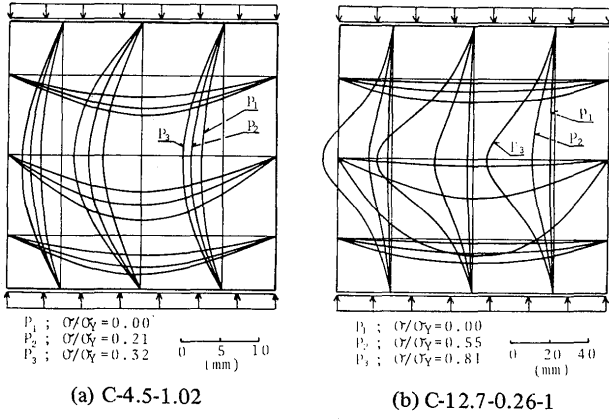


Fig. 5 Shapes of deflection under loading

Also Figs. 6(a) and (b) show the typical compressive stress distributions at the middle section of the plate for a thin plate, C-4.5-1.28RS and a thick plate, C-9.0-0.71RS, respectively. In the case of a thin plate, comparatively large deflection is produced even from the beginning of loading, and the load is supported mainly by the effective portions appeared along the sides of the plate. In the case of a thick plate, the deflection is not so large until plastic zone appears and the load is carried at all parts of the plate width. But, as the load increases, the local plastification produces a rapid increase in the deflection at the central portion of the plate and the additional load becomes to be supported mainly by the effective portion of the plate, as seen in the case of a thin plate.

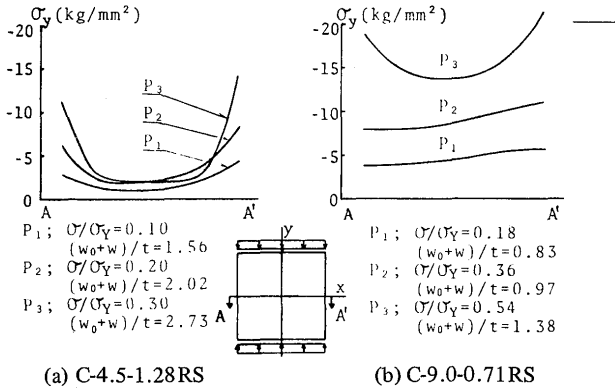


Fig. 6 Stress distribution under loading

3. Formulation of the elastic-plastic large deflection analysis by the Finite Element Method.

To analyse the behavior of the plates under compression, the finite element method is used considering both material and geometrical nonlinearities applying the incremental procedure. In this section, the formulation of this analysis developed by the authors is presented.

3.1 Stress-strain relation

(a) Elastic range

If the material is in the elastic range, the relation between the stress increments $\{d\sigma\}$ and the strain increments $\{d\epsilon\}$ is expressed with the elasticity matrix $[D^e]$ in the following form

$$\{d\sigma\} = [D^e] \{d\epsilon\} \quad (1)$$

(b) Plastic range

The material yields if a scalar function $f(\sigma_x, \sigma_y, \sigma_z, \tau_{xy}, \tau_{yz}, \tau_{zx})$ reaches the value of the function $f_0(\sigma_Y, \kappa)$, where σ_Y is the yield stress and κ is the plastic hardening parameter,

$$F = f - f_0 = 0 \quad (2)$$

F in the above equation is called the yield function. According to the hypothesis of the theory of plasticity, the plastic strain increments show incompressibility. Assuming that the yield function is a plastic potential, the plastic strain increments $\{d\epsilon_p\}$ are expressed in the form

$$\{d\epsilon_p\} = d\lambda \left\{ \frac{\partial f}{\partial \sigma} \right\} \quad (3)$$

where $d\lambda$ is a scalar factor of proportionality. The total strain increments $\{d\epsilon\}$ which are the sum of the elastic strain increments $\{d\epsilon_e\}$ and the plastic strain increments $\{d\epsilon_p\}$ become

$$\{d\epsilon\} = \{d\epsilon_e\} + \{d\epsilon_p\} = \{d\epsilon_e\} + d\lambda \left\{ \frac{\partial f}{\partial \sigma} \right\} \quad (4)$$

The stress increments $\{d\sigma\}$ are given by replacing $\{d\epsilon\}$ with $\{d\epsilon_e\}$ in Eq. (1), that is

$$\{d\sigma\} = [D^e] \{d\epsilon_e\} = [D^e] \left(\{d\epsilon\} - d\lambda \left\{ \frac{\partial f}{\partial \sigma} \right\} \right) \quad (5)$$

If the material is under loading in the plastic range, the increment of f must be equal to that of the value of f_0 . This gives

$$df = df_0 \quad (6)$$

Assuming that the plastic hardening parameter κ is of a function of the plastic strains, Eq.(6) becomes

$$\left\{ \frac{\partial f}{\partial \sigma} \right\}^T \{d\sigma\} = \left(-\frac{\partial f_0}{\partial \kappa} \right) \left\{ \frac{\partial \kappa}{\partial \epsilon_p} \right\}^T \{d\epsilon_p\} \quad (7)$$

Substituting Eq.(5) into Eq.(7), $d\lambda$ is solved as,

$$d\lambda = \frac{\left\{ \frac{\partial f}{\partial \sigma} \right\}^T [D^e] \{d\epsilon\}}{\left\{ \frac{\partial f}{\partial \sigma} \right\}^T [D^e] \left\{ \frac{\partial f}{\partial \sigma} \right\} + \left(-\frac{\partial f_0}{\partial \kappa} \right) \left\{ \frac{\partial \kappa}{\partial \epsilon_p} \right\}^T \left\{ \frac{\partial f}{\partial \sigma} \right\}} \quad (8)$$

From Eqs. (5) and (8), the relation between the stress increments and the strain increments in the plastic range

is expressed in the form

$$\{d\sigma\} = [D^p] \{d\epsilon\} \quad (9)$$

where

$$[D^p] = [D^e] - \frac{1}{S} [D^e] \left\{ \frac{\partial f}{\partial \sigma} \right\} \left\{ \frac{\partial f}{\partial \sigma} \right\}^T [D^e] \quad (10)$$

$$S = \left\{ \frac{\partial f}{\partial \sigma} \right\}^T [D^e] \left\{ \frac{\partial f}{\partial \sigma} \right\} + \left(\frac{\partial f_0}{\partial \kappa} \right) \left\{ \frac{\partial \kappa}{\partial \epsilon} \right\}^T \left\{ \frac{\partial f}{\partial \sigma} \right\}$$

On the course of computation, loading or unloading of the material element in the plastic range is distinguished by the following conditions,

$d\lambda > 0$; loading, $d\lambda = 0$; neutral loading, $d\lambda < 0$; unloading. When unloading is detected for a certain load increment, the stress-strain relations should be replaced by Eq.(1) instead of Eq.(9).

3.2 Deformation-strain relation

For the analysis of large deformation of structures, a characterisitic deformation-strain relation should be defined. In this section, it will be represented explicitly in matrix form for a plate element.

A set of local coordinates is fixed on each finite element throughout the entire course of deformation and the behavior of the structure is described in reference to the global coordinates. The deformation of the element is denoted by $\{h\}$ which consists of in-plane displacements $\{s\}$ and lateral displacements $\{w\}$, that is

$$\{h\} = [s, w]^T \quad (11)$$

These components of displacements $\{s\}$ and $\{w\}$ can be expressed by the nodal displacements $\{s_n\}$ and $\{w_n\}$, and the displacement function $[A_p]$ and $[A_b]$ in the element. Thus,

$$\begin{aligned} \{s\} &= [A_p] \{s_n\} \\ \{w\} &= [A_b] \{w_n\} \end{aligned} \quad (12)$$

The components of the nodal displacements are as follows. $\{s_n\} = [u_n, v_n]^T$

$$\{w_n\} = [w_n, \left(\frac{\partial w}{\partial x}\right)_n, \left(\frac{\partial w}{\partial y}\right)_n]^T \quad (13)$$

According to the theory of elasticity, the strains in the plate element are expressed in the following form.

$$\{\epsilon\} = \begin{Bmatrix} \epsilon_x \\ \epsilon_y \\ \epsilon_{xy} \end{Bmatrix} = \begin{Bmatrix} \frac{\partial u}{\partial x} \\ \frac{\partial v}{\partial y} \\ \frac{\partial v}{\partial x} + \frac{\partial u}{\partial y} \end{Bmatrix} + \frac{1}{2} \begin{Bmatrix} \left(\frac{\partial w}{\partial x}\right)^2 \\ \left(\frac{\partial w}{\partial y}\right)^2 \\ 2 \frac{\partial w}{\partial x} \frac{\partial w}{\partial y} \end{Bmatrix}$$

$$-z \begin{Bmatrix} \frac{\partial^2 w}{\partial x^2} \\ \frac{\partial^2 w}{\partial y^2} \\ 2 \frac{\partial^2 w}{\partial x \partial y} \end{Bmatrix} \quad (14)$$

$$= [B_p] \{s_n\} + \frac{1}{2} [C_0] [B_{b1}] \{w_n\} - z [B_{b2}] \{w_n\}$$

In Eq.(14), the first term indicates the in-plane strains, the second represents additional membrane strains due to large deflection, and the third term shows the strains due to bending. The second term exhibits the geometrical nonlinearity of the behavior, expressed by a square of the bending slope of the element. $[B_p]$, $[B_{b1}]$ and $[B_{b2}]$ are obtained by partially differentiating the displacement functions $[A_p]$ and $[A_b]$, and $[C_0]$ is expressed in the form

$$[C_0] = \begin{Bmatrix} \frac{\partial w}{\partial x} & 0 \\ 0 & \frac{\partial w}{\partial y} \\ \frac{\partial w}{\partial y} & \frac{\partial w}{\partial x} \end{Bmatrix} \quad (15)$$

Now, let Eq.(14) express the strains at a certain loading state $\{F\}$. After the load increment $\{dF\}$, the strains change to $\{\epsilon + d\epsilon\}$. Thus the strains at the loading state $\{F + dF\}$ become

$$\begin{aligned} \{\epsilon + d\epsilon\} &= [B_p] \{s_n + ds_n\} + \frac{1}{2} [C_0 + dC_0] \\ &\quad [B_{b1}] \{w_n + dw_n\} - z [B_{b2}] \{w_n + dw_n\} \end{aligned} \quad (16)$$

Therefore, the strain increments $\{d\epsilon\}$ are obtained by subtracting Eq.(14) from Eq.(16). That is,

$$\begin{aligned} \{d\epsilon\} &= [B_p] \{ds_n\} + [C_0] [B_{b1}] \{dw_n\} \\ &\quad + \frac{1}{2} [dC_0] [B_{b1}] \{dw_n\} - z [B_{b2}] \{dw_n\} \end{aligned} \quad (17)$$

Here, virtual strain increments $\{\delta d\epsilon\}$ which are necessary for applying the principle of virtual work is calculated at the loading state $\{F + dF\}$. At this state, if arbitrary virtual displacements $\{\delta dh\}$ are imposed, the corresponding strain increments $\{\delta d\epsilon\}$ are in the form

$$\begin{aligned} \{\delta d\epsilon\} &= [B_p] \{\delta ds_n\} + [C_0 + dC_0] [B_{b1}] \{\delta dw_n\} \\ &\quad - z [B_{b2}] \{\delta dw_n\} \end{aligned} \quad (18)$$

The deformation-strain relation defined in the above is given in the local coordinates fixed to the element. However, this local coordinate system moves as the total structure deforms. So, it is necessary to transform this local coordinates to the global coordinates at each loading step when the equilibrium of the total structure is constructed. Denoting $[\Lambda]$ as the transformation matrix of the coordinates and $\{h_g\}$ as the displacements in the global coordinates, the displacements $\{h\}$ in the local coordinates are expressed in the form

$$\{h\} = [\Lambda] \{h_g\} \quad (19)$$

3.3 Equilibrium equation

At a certain loading state, the external load $\{F_g\}$ is acting on the structure, and the stresses $\{\sigma\}$ are produced. With a load increment $\{dF_g\}$, the stresses are changed by $\{d\sigma\}$. The equilibrium condition of the structure corresponding to this state will be obtained by applying the principle of virtual work.

According to this principle, the virtual work δU done by the internal forces must be equal to the virtual work δW done by the external loads, that is

$$\delta U = \delta W \quad (20)$$

Explicit form of the above is derived in the following.

The internal work of the whole structure is obtained as a sum of the internal work ΔU^e of an individual element, which is expressed in the form

$$\delta U^e = \int \{ \delta d\epsilon \}^T \{ \sigma + d\sigma \} dV \quad (21)$$

Using the stress-strain relation to this equation, Eq.(21) becomes

$$\delta U^e = \int (\{ \delta d\epsilon \}^T \{ \sigma \} + \{ \delta d\epsilon \}^T [D] \{ d\epsilon \}) dV \quad (22)$$

where

$$[D] = \begin{cases} [D^e] ; \text{elastic} \\ [D^p] ; \text{plastic} \end{cases} \quad (23)$$

Substituting Eqs.(17) and (18) into Eq.(22), the internal work is expressed in the form

$$\begin{aligned} \delta U^e &= \begin{Bmatrix} \delta ds_n \\ \delta dw_n \end{Bmatrix}^T \begin{bmatrix} K_{pp} & K_{pb} \\ K_{bp} & K_{bb} \end{bmatrix} \begin{Bmatrix} ds_n \\ dw_n \end{Bmatrix} + \begin{Bmatrix} \delta ds_n \\ \delta dw_n \end{Bmatrix}^T \begin{Bmatrix} R_p \\ R_b \end{Bmatrix} \\ &= \{ \delta dh_n \}^T [K]^e \{ dh_n \} + \{ \delta dh_n \}^T \{ R \}^e \quad (24) \end{aligned}$$

where

$$[K_{pp}] = \int [B_p]^T [D] [B_p] dV$$

$$[K_{pb}] = [K_{bp}]^T = \int ([B_p]^T [D] [C_0] [B_{b1}] - z [B_p]^T$$

$$[D] [B_{b2}]) dV$$

$$\begin{aligned} [K_{bb}] &= \int (z^2 [B_{b2}]^T [D] [B_{b2}] + [B_{b1}]^T [P] [B_{b1}] \\ &+ [B_{b1}]^T [C_0]^T [D] [C_0] [B_{b1}] - z [B_{b1}]^T [C_0]^T [D] [B_{b2}] \\ &- z [B_{b2}]^T [D] [C_0] [B_{b1}]) dV \\ \{ R_p \} &= \int [B_p]^T \{ \sigma \} dV \\ \{ R_b \} &= \int ([B_{b1}]^T [C_0]^T - z [B_{b2}]^T) \{ \sigma \} dV \\ [P] &= \begin{bmatrix} \sigma_x & \tau_{xy} \\ \tau_{xy} & \sigma_y \end{bmatrix} \end{aligned} \quad (25)$$

The displacement increments in the local coordinates can be transformed to those in the global ones, with the aid of the transformation matrix $[\Lambda]$ defined in Eq.(19). Thus, the internal work δU^e for the element becomes

$$\delta U^e = \{ \delta dh_g \}^T [K_g]^e \{ dh_g \} + \{ \delta dh_g \}^T \{ R_g \}^e \quad (26)$$

where

$$[K_g]^e = [\Lambda]^T [K]^e [\Lambda] \quad (27)$$

$$\{ R_g \}^e = [\Lambda]^T \{ R \}^e [\Lambda]$$

The internal work of the whole structure is then obtained as follows.

$$\begin{aligned} \delta U &= \sum \delta U^e \\ &= \{ \delta dh_g \}^T [K_g] \{ dh_g \} + \{ \delta dh_g \}^T \{ R_g \} \end{aligned} \quad (28)$$

Next, the virtual work done by the external loads $\{F_g + dF_g\}$ during the virtual displacement $\{ \delta dh_g \}$ is expressed in the form

$$\delta W = \{ \delta dh_g \}^T \{ F_g + dF_g \} \quad (29)$$

In reference to Eq.(20), Eq.(29) should be equal to Eq.(28). Thus, the equilibrium equation is

$$\{ F_g + dF_g \} = [K_g] \{ dh_g \} + \{ R_g \} \quad (30)$$

or

$$\{ dF_g \} + \{ L_g \} = [K_g] \{ dh_g \} \quad (31)$$

and

$$\{ L_g \} = \{ F_g \} - \{ R_g \} \quad (32)$$

Eq.(31) predicts the increments of displacement as the first approximation, but this does not guarantee equilibrium at the newly displaced position, since the equilibrium equation is linearized. When the load increment is assumed to be zero, only the vector $\{L_g\}$ remains in the equation as the load.

$$\{ L_g \} = [K_g] \{ dh_g \} \quad (33)$$

$\{L_g\}$ can be regarded as a correction load to improve the approximate equilibrium.

4. Analysis by the Finite Element Method

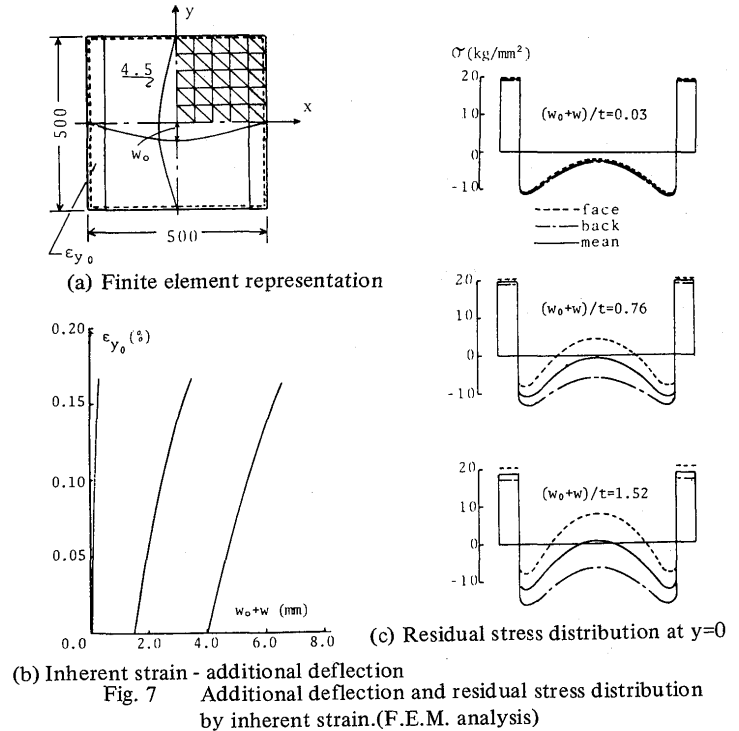
The element which is used in the following analysis is a triangular element with a right angle, and is fictitiously divided into 20 layers to calculate stresses. The stresses at the center of each layer are represented as the stress state in the layer. In evaluation of the stiffness matrix, the integration to z direction is carried out numerically at 20 points (the center of each layer) using the corresponding stress-strain relation.

4.1 Relation between welding residual stresses and initial deformation

Welded structures are always accompanied by welding residual stresses and initial deformation, and there are generally a close relation between them. Here, restricting the problem to the case of plate elements in welded structures, initial deflection is produced primarily by thermal angular distortion of fillet weldment laid to fit flanges or stiffeners to panels along their edges. Then, additional deflection is produced by the compressive residual stresses due to shrinkage of the plate near the welding bead. In this section, a relation between in-plane compressive stresses and out-of-plane deformation is studied for a simply supported square plate of 500x500mm which was furnished in the preceding experiment

First, it is assumed that the plate has originally initial deflection of a sinusoidal wave for some reasons, and then weld metal is laid along two parallel edges. In analysis, the shrinkage in the plate after welding is replaced by inherent strains which are imposed in the portions $1/10$ of the plate breadth along both edges as shown in Fig.7(a). The inherent strains are applied incrementally until these edge portions become plastic in tension. The relations between the imposed inherent strains and the central deflection, and the distribution of the residual stresses along $y=0$ are shown in Figs.7(b) and (c) for the plate of 4.5mm thickness. When the original initial deflection is large, the additional deflection due to the in-plane residual stresses becomes also large. Due to this additional deflection, the compressive residual stresses at the center of the plate decrease in comparison with the case of a flat plate, and the local bending stresses become large.

The calculated distribution of residual stresses shown in Fig.7(c) coincide well with the measured one shown in Fig.2, both in the tendency and the magnitude. Thus, it is seen that welding residual stresses can be estimated by this inherent strain method and those of

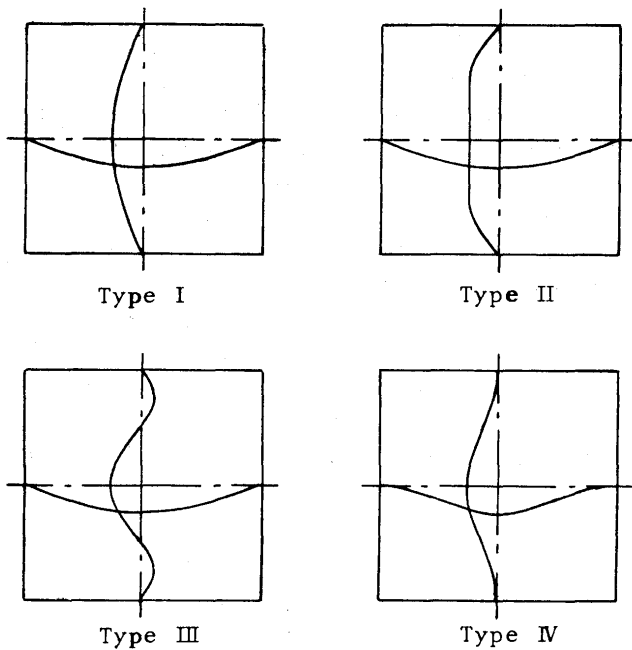


4.2 Effect of the shape of initial deflection

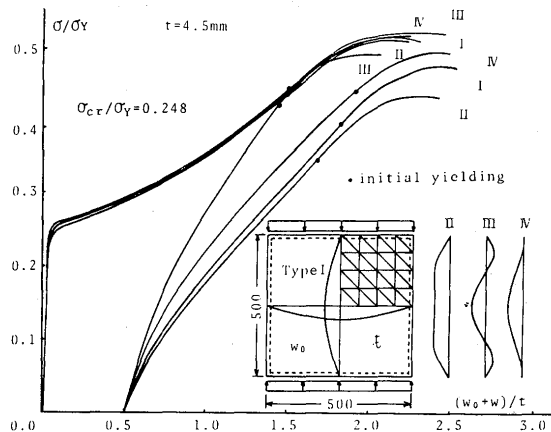
Concerning the effect of initial deflection on the rigidity and strength of plates, there are two factors which should be considered; the shape and the magnitude of initial deflection. In order to clarify on influence of the shape of initial deflection, four types of initial deflections for plates of 4.5mm and 9.0mm thickness are assumed in the analysis shown in Fig.8(a), the magnitude of deflection at the center of the plate being kept the same; 0.01 and 0.5 times the plate thickness. The plates are assumed to be simply supported along their four edges, and the loads are applied so as to give a uniform displacement on the loading edges.

Fig.8(b) shows the relation between the average compressive stress and the deflection at the center for 4.5mm thickness plate. In the same figure, the finite element representation is also shown.

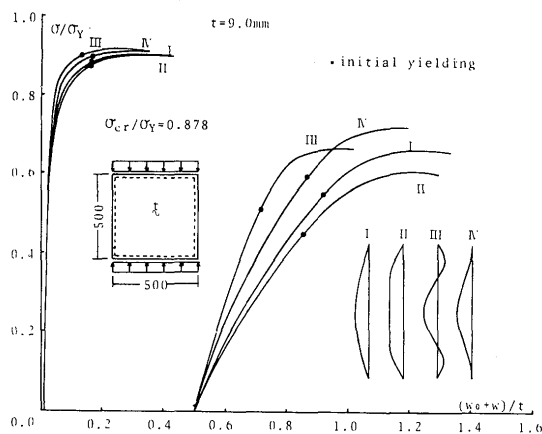
When the magnitude of initial deflection is small, the difference of the shape of initial deflection has a very little influence on the rigidity and strength of the plates. However, when it is large, there exists noticeable differences in the behavior of the plates such that, the larger the volume occupied between the initial surface of the middle plane of the plate and the flat plane containing its four corners are, the lower the rigidity and the ultimate strength become. This is due to the fact that larger bending moment at each point of the plate is produced by larger deflection under a certain amount of compressive load. However, the ultimate strength for all types of shape and any magnitude of initial deflection would never exceed the ultimate strength of the flat plate.



(a) Different shapes of initial deflection for F.E.M. analysis



(b) Applied compressive stress - central deflection for $t=4.5\text{mm}$



(c) Applied compressive stress - central deflection for $t=9.0\text{mm}$

Fig. 8 Effect of the shape of initial deflection

Fig.8(c) also show the results of the plate of 9.0mm thickness, and the same tendency can be observed as in the previous case.

4.3 Comparison with the test results

In order to examine the validity of the analysis, the results of the elastic-plastic large deflection analysis are compared with the test results presented in section 2.4. In the analysis, the loading and supporting conditions are the same as those in the experiment, and the plates are given a sinusoidal shape of initial deflection.

Fig.9 shows the relation between the mean compressive stress and central deflection based on the results of both experiments and analyses for some specimens. In the case of thicker plates, both results are almost coincided. On the other hand, for the thin plate in these examples, some differences are observed between the results of experiment and analysis. This may be attributed to the difference of the shape of actual initial deflection from the assumed one in the analysis, since the formation of initial deflection is not well controlled in the case of thin plates. It may be concluded that this analysis can well describe the actual behavior of the plate.

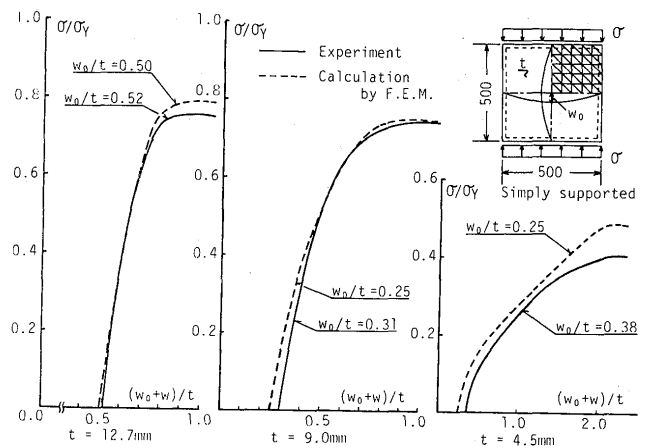


Fig. 9 Comparison of the results of F.E.M. analysis with experimental results

4.4 Effects of magnitude of initial deflection and welding residual stresses

First, in order to clarify the effect of the magnitude of initial deflection a series of analysis is performed on 500x500 mm square plates of which thicknesses are 4.5mm, 9.0mm and 12.7mm. The plates are assumed to be simply supported along the four edges. The shape of initial deflection is assumed of a sinusoidal wave, and the ratios of the maximum deflection to the plate thickness are chosen as 0.01, 0.25, 0.50 and 1.00 for each plate thickness. Later, the analysis is continued to carry out on the same plates which have both the initial deflection and the welding residual stresses which are produced by the inherent strain method mentioned in section 4.1.

Load-displacement curves and load-deflection curves with a variation in the magnitude of initial deflection are shown for each plate thickness in Figs.10(a) to (c), and Figs.11(a) to (c), respectively. The finite element representation used for the analysis is also shown in these figures. The full line curves represent the results considering only the initial deflection and the dotted line curves containing both the welding residual stresses and initial deflection.

The slope of the load-displacement (applied stress and average strain) curve indicates the compressive rigidity of a plate. In the case of a thin flat plate as seen in Fig.10(a), the rigidity is equal to Young's modulus, E , of the material, under a small amount of load, but as the load increases, the buckling occurs and the rigidity decreases to about a half of E , and a plate with small initial deflection exhibits a similar behavior. When the initial deflection is large, the rigidity is smaller than E from the beginning of the loading, but after the buckling load is reached, it becomes also to about a half of the ordinary

Young's modulus, E . Then as the load increases, local yielding occurs, and the rigidity gradually decreases to zero when the plate reaches its ultimate strength. Fig.10(a) also shows the decrease of the rigidity due to the welding residual stresses. In the case of a thicker plate shown in Figs.10(b) and (c), the rigidity is first equal to its Young's modulus, E , of the material, but after the yielding occurs at a high value of σ/σ_Y , it suddenly decreases and the fatal collapse occurs, when the initial deflection is small. On the other hand, when the initial deflection is large, the rigidity is smaller than E from the beginning of the loading, but keeps nearly constant values relating to the magnitude of initial deflection. After yielding occurs

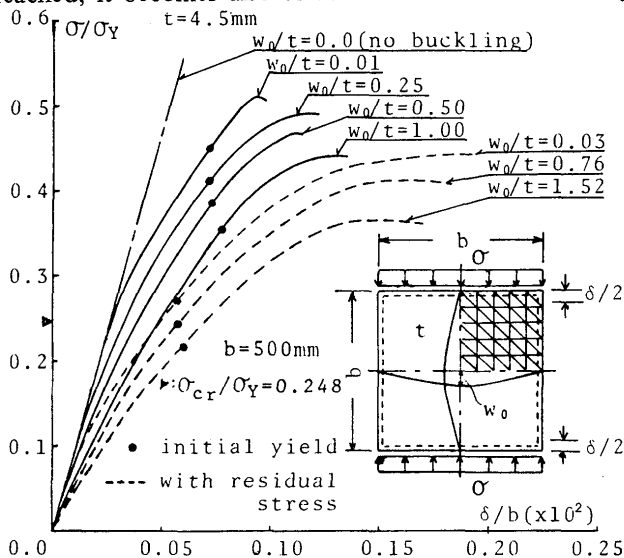
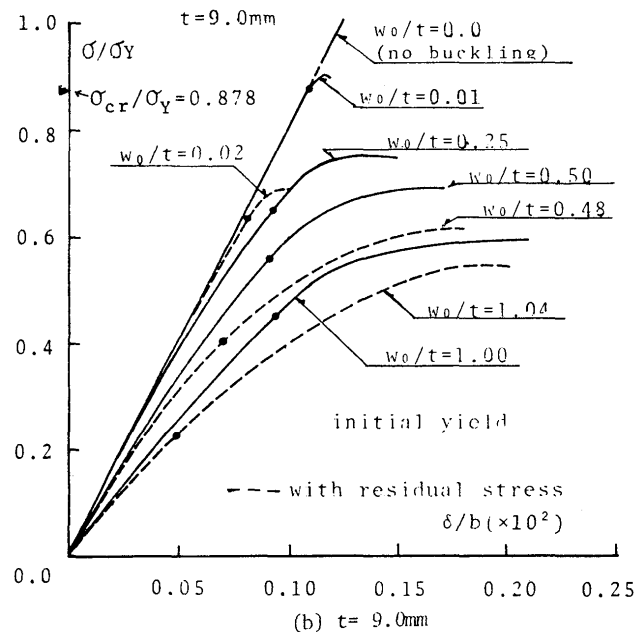
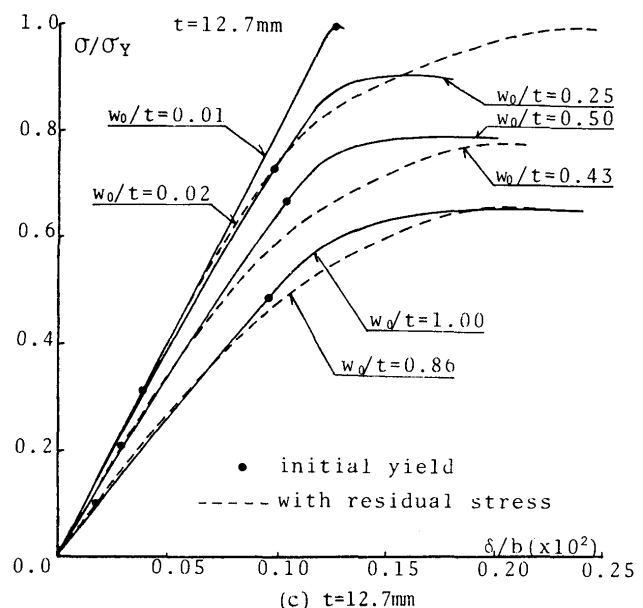
(a) $t = 4.5\text{mm}$

Fig. 10

Applied compressive stress - compressive displacement curves. (F.E.M. analysis)

(b) $t = 9.0\text{mm}$ (c) $t = 12.7\text{mm}$

at a lower value of σ/σ_Y , it gradually decreases to zero, and the load reaches the maximum. The welding residual stresses also decrease the rigidity of the plates.

These behaviors are also observed from the load-deflection curves shown in Figs.11(a), (b) and (c). Especially, Fig.11(a) shows the remarkable decrease of the buckling load due to the existence of the welding residual stresses. The ultimate strength is reduced by the initial deflection, and this decrease is more remarkable when the plate thickness is larger as understood from Fig.10 or Fig.11. As also indicated by the test results in section 2.4, the effective portions to carry the load become small from the beginning of the loading, when the initial deflection is large. This causes the decrease in

the ultimate strength.

When the plate is thin, the deflection due to the compressive load is large as compared with its thickness. But plastification is delayed because the thin plate is more flexible. In contrast with this, the deflection of the thick plate due to the compressive load is not so large as compared with its thickness. But plastification occurs for a relatively smaller deflection. This plastification cause the remarkable decrease in the ultimate strength of thick plate due to the initial deflection as compared with the thin plates.

Welding residual stresses also decrease the ultimate strength in general. As to the effects of welding residual stresses, they may be divided into two which are the tensile and compressive residual stresses. The tensile residual stress field is generally produced along the edges of the plate, and these portions often coincide with the effective portion to carry the compressive load. So, these tensile residual stresses delay the plastification of these parts and increase the ultimate strength under compression. On the other hand, the compressive stress field in the middle of the plate increases the deflection and also promote local plastification. So, this compressive residual stresses decrease the ultimate strength under compression. Under these two contradictory effects, the decrease in the compressive ultimate strength due to the welding residual stresses is most remarkable when the ratio of the plate breadth to the plate thickness, b/t is about 50 to 60.

4.5 Ultimate strength obtained by analysis and experiment

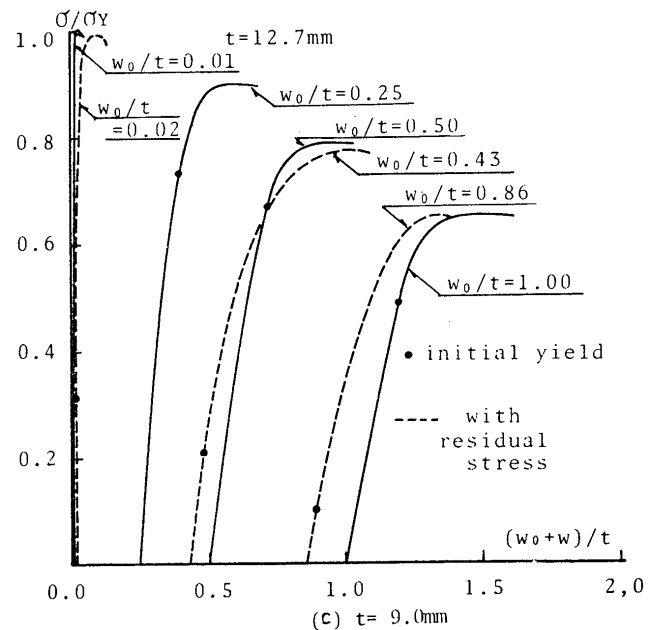
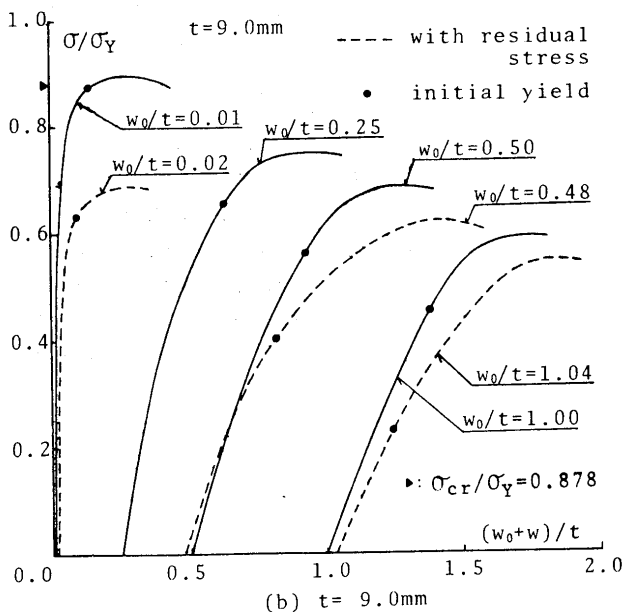
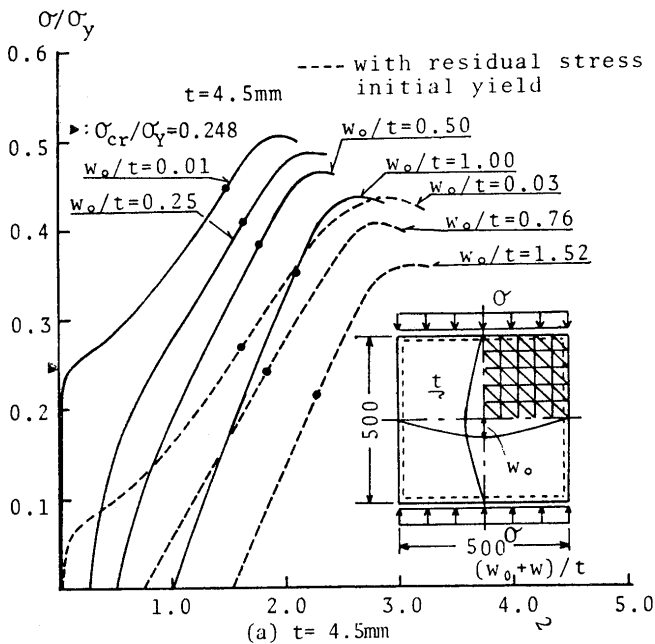


Fig. 11 Applied compressive stress - central deflection curves. (F.E.M. analysis)

The ultimate strength of square plates under compression obtained by the elastic-plastic large deflection analyses and the experiments are represented in Figs.12(a), (b) and (c), for the plate thicknesses being 4.5mm, 9.0mm and 12.7mm, respectively, with respect to the ratio of the maximum initial deflection to the plate thickness, w_0/t . The calculated curves are a little higher than the experimental ultimate strength for the plates of 4.5mm and 12.7mm thickness. However, taking into account of a sensible character of the behavior of the plates such as the load condition, the effect of local plastification of the plates during the process of forming

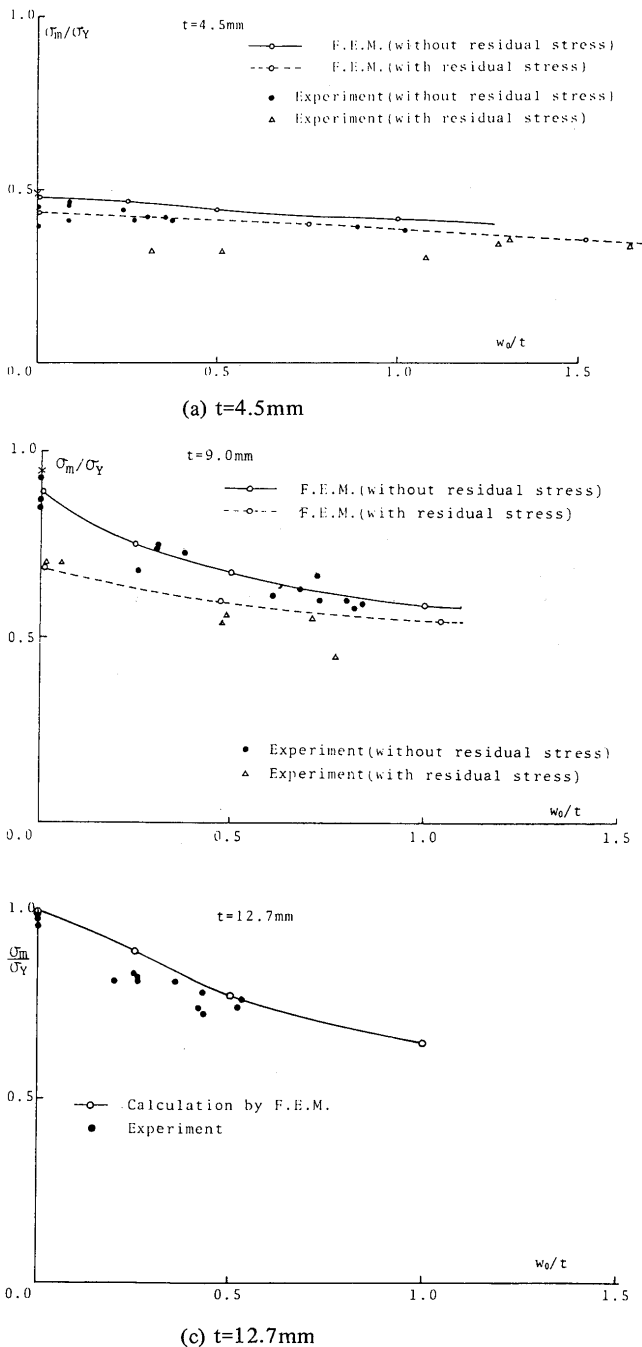


Fig. 12 Relation between compressive ultimate strength and initial deflection including residual stresses.

initial deflection and the difference of the shape of initial deflection between the experiments and the analyses, it can be said that both results are well coincide for all cases.

Concerning the ultimate strength of a plate with no imperfection subjected to compression, Von Kármán¹⁵⁾ proposed the concept of the effective width. According to this concept, the ultimate strength is expressed in the form

$$\frac{\sigma_m}{\sigma_Y} = \frac{\pi}{\sqrt{3(1-\nu^2)}} \frac{t}{b} \sqrt{\frac{E}{\sigma_Y}} \quad (34)$$

where t and b are the plate thickness and breadth, respectively. The calculated value of this equation is also presetned in Figs.12(a) and (b) by \times . These values are close to those evaluated by F.E.M. in thin plate, but rather higher than those in thicker plates. The ultimate strength predicted by Von Kármán can be regarded as higher ultimate strength of a plate with no initial deflection.

Finally, summarizing all results, the ultimate strength is presented against the breadth to thickness ratio, $b/t \sqrt{\sigma_Y/E}$ in Fig.13. The buckling strength curve and the Von Kármán's ultimate strength curve are also added in the same figure. As mentioned in section 4.4, the more reduction in the ultimate strength due to the initial deflection is observed for the thicker in plate thickness, and decrease of the ultimate strength due to the welding residual stresses is most predominant when the value of $b/t \sqrt{\sigma_Y/E}$ is about 2.0 (b/t is 50 to 60).

4.6 Effect of local bending stresses

In the preceding analyses, the consequent bending stresses due to the initial deflection are not accounted. As for the analysis of the experiment, it is not necessary to take account of these bending stresses in these special cases. This is because that the initial deflection of the specimen is formed by the press machine producing plastic deformation in the plate, and after the press load is removed, the resulting local bending stresses should be very small, and must be in equilibrium as a whole plate. In contrast with this, in the case of actual structural elements, the initial deflection is produced mainly by the angular distortion of fillet weldments and the compressive residual stresses due to this welding, and the local bending stresses accompanied to this initial deflection can not be ignored especially when the magnitude of this initial deflection is large. In this section, an influence of these local bending stresses upon the rigidity and strength of the square plates under compression is examined. First, in order to produce both initial deflection and bending

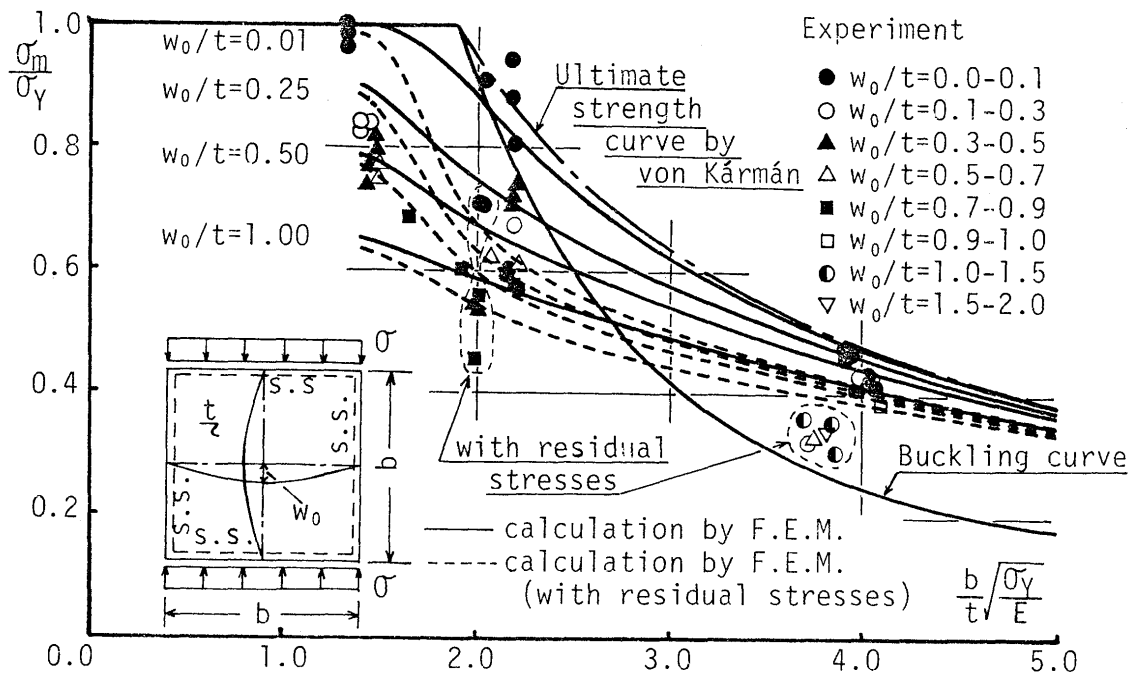


Fig. 13 Compressive ultimate strength of square plates including effects of initial deflection and welding residual stresses.

stresses similar to actual cases, uniformly distributed bending moments are applied along the four edges of the 500 x 500mm square plate of 4.5mm thickness.

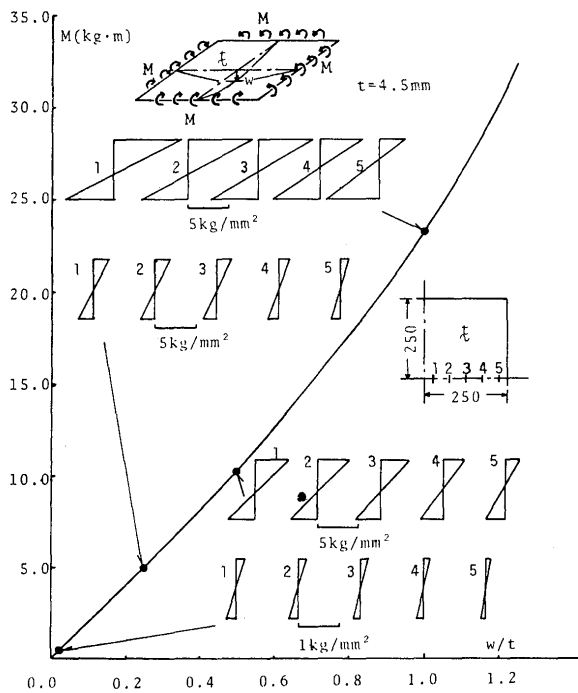


Fig. 14 Uniformly distributed end moment - central deflection curve. (F.E.M. analysis)

Fig.14 shows the relation between the applied moment and the deflection at the center of the plate, and the distribution of the bending stresses. It is seen that the accompanied bending stresses in the extreme fibers are about $\pm 7\text{kg/mm}^2$ in magnitude when the initial deflection at the center of the plate is close to its

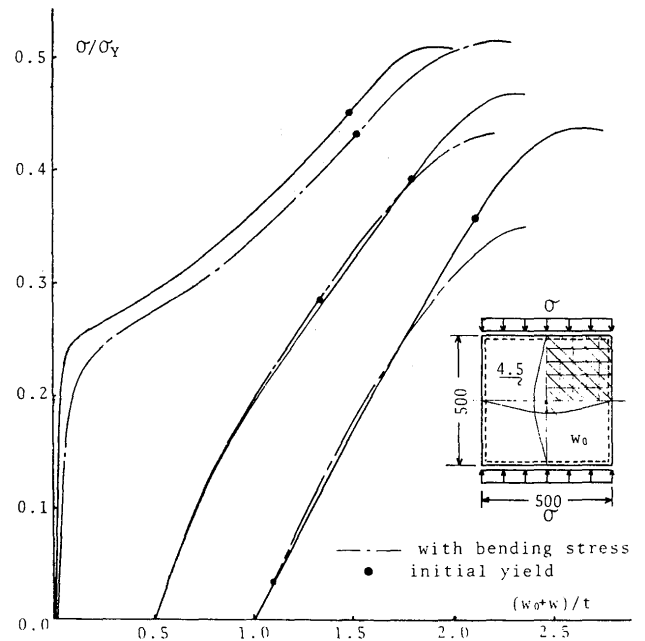


Fig. 15 Effect of bending stresses induced by initial deflection upon ultimate strength. (F.E.M. analysis)

thickness. With these initial deflection with the bending stresses as the initial condition, the behavior of the square plate under compression is analysed. Fig.15 shows the relation between the mean compressive stress and the central deflection of the plate, in which full lines indicate the results with initial deflection only and the chain lines results with initial deflection only and the chain lines those with both initial deflection and bending stresses. It is found that local plastification takes place at the earlier stage of loading due to the superposition of the initial local bending stresses and the applied compressive stresses, and this causes the decrease of the ultimate strength, especially in the case of larger initial deflection. Thus, due attention should be paid to the effect of the local bending stresses accompanied by the initial deflection, when initial deflection is large.

6. Conclusion

A series of elastic plastic large deflection analyses using the finite element method are conducted for the simply supported square plates under compression to clarify the effects of the shape and the magnitude of initial deflection, and the effect of the welding residual stresses. Two series of experiments are also carried out for the same purpose. The result obtained are as follows.

- (1) Results of the analysis by the finite element method and the experiment show good agreement. Also the ultimate strength predicted by Von Kármán is close to but rather higher than these results even in the case of no imperfection.
- (2) The difference of the shape of initial deflection has a very little influence upon the rigidity and ultimate strength in the case of small initial deflection. When initial deflection becomes large, there exist some differences in the behavior of the plates. However, the ultimate strength for all types of shape and any magnitude of initial deflection would never exceed the ultimate strength of the flat plate.
- (3) In the case of a thin plate which buckles elastically, the rigidity after buckling becomes to about a half of Young's modulus, E , of the material, which should originally equal to E , for small initial deflection. The initial deflection decreases the rigidity, but the rigidity above the buckling load becomes about a half of E regardless to the magnitude of initial deflection.
- (4) In the case of a thick plate which does not buckles elastically, the rigidity decreases suddenly after the local yielding takes place, for small initial deflection. When initial deflection is large, the rigidity is not high originally, and gradually decreases after the local yielding.
- (5) Initial deflection decreases the ultimate strength of the plate under compression, and this decrease is more remarkable when the plate is thicker.
- (6) The welding residual stresses decrease the rigidity and the ultimate strength in general, and this decrease is most remarkable when $b/t\sqrt{\sigma_Y/E} \div 2.0$.
- (7) The bending stresses which are accompanied by the initial deflection also decrease the ultimate strength, and this decrease can not be ignored when initial deflection is large.

7. Acknowledgements

This study was sponsored by the Japan Ship Research Association under project SR.127. The authors are thankful to Dr. Fujita, the chairman, and the members of SR.127, for their valuable discussions. Many thanks are due to Messrs Sasada, Koki and Kotake who helped in the experimental work, and to Messrs Murakawa and Kikumoto for their helpful cooperations.

References

- 1) Y. Yamamoto: "Initial Deflection and Plastic Buckling", J. Soc. Naval Arch., Vol.97 (1955), p.57. (in Japanese)
- 2) M. Yoshiki, Y. Akita and N. Ando: "Buckling and Corrugation of Continuous Panel with Initial Deflection", J. Soc. Naval Arch., Vol.101 (1957), p.137. (in Japanese)
- 3) Y. Fukumoto: "Rigidity of Continuous Panel with Initial Deflection (2nd Report)", J. Soc. Naval Arch., Vol.109 (1961), p.289. (in Japanese)
- 4) M. Yoshiki, Y. Fujita and T. Kawai: "Influence of Residual Stresses on the Buckling of Plates", J. Soc. Naval Arch., Vol.107 (1960), p.187. (in Japanese)
- 5) Y. Fujita and K. Yoshida: "Plastic Design in Steel Structures (4th Report) - Influence of Residual Stresses on the Plate Instability -", J. Soc. Naval Arch., Vol.115 (1963), p.106. (in Japanese)
- 6) Y. Ueda, W. Yasukawa and M. Uenishi: "Inelastic Local Buckling of Built-Up I-Section", Technical Reports of the Osaka University, Vol.16, No.737. (1966)
- 7) Y. Ueda and L. Tall: "Inelastic Buckling of Plates with Residual Stresses", International Association for Bridge and Structural Engineering, Zurich. (1967)
- 8) Y. Ueda: "Local Buckling", in Special Report "Welding Residual Stresses and Buckling Strength", JSSC (Japan Society of Steel Construction), Vol.3, No.16 (1967), p.27, p.49. (in Japanese)
- 9) H. Ohtsubo: "A General Method of Analysis of Large-Deformed Elastic-Plastic Plate Problems", J. Soc. Naval Arch., Vol.130 (1971), p.173. (in Japanese)
- 10) H. Okamura and K. Yoshida: "Ultimate Strength of Rectangular Shell plates in Edge Compression", Trans. JSCE, Vol.206 (1972), p.1. (in Japanese)
- 11) Y. Ueda, T. Yamakawa and A. Fujiwara: "Analysis of Thermal Elastic-Plastic Large Deflection of Columns and Plates by Finite Element Method", JSSC, 7th Symposium on Matrix Method (1973), p.411. (in Japanese)
- 12) H. Arai: "Analysis on the Large Deformation of Plate Structures (1st Report)", J. Soc. Naval Arch., Vol.134 (1973), p.269. (in Japanese)

- 13) Y. Ueda, W. Yasukawa, T. Yao, H. Ikegami and R. Ohminami: "Ultimate Strength of Square Plates Subjected to Compression (1st Report) –Effects of Initial Deflection and Welding Residual Stresses–", J. Soc. Naval Arch., Vol.137 (1975), p.315. (in Japanese)
- 14) F. Nishioka, K. Nishimaki, M. Matsuishi, T. Tanaka, W. Yasukawa, T. Yamauchi and O. Tohogoh: "On Automatic Bending of Plates by the Universal Press with Multiple Piston Heads", J. Soc. Naval Arch., Vol.132 (1972), p.481. (in Japanese)
- 15) T. Von Kármán, E. E. Sechler and L. H. Donnell: "The Strength of Thin Plates in Compression", Trans. ASME, Vol.54 (1932), p.53.